INL/CON-16-39871
PREPRINT

SINGLE PHASE ANALYTICAL MODELS FOR TERRY TURBINE NOZZLE

2017 International Congress on Advances in Nuclear Power Plants (ICAPP2017)

Haihua Zhao, Hongbin Zhang, Ling Zou, James O'Brien

November 2016

SINGLE PHASE ANALYTICAL MODELS FOR TERRY TURBINE NOZZLE

Haihua Zhao, Hongbin Zhang, Ling Zou, James O'Brien

Idaho National Laboratory, P.O. Box 1625, Idaho Falls, ID, 83415-3870, USA
haihua.zhao@inl.gov

As part of the efforts to understand the unexpected "self-regulating" mode of the RCIC (Reactor Core Isolation Cooling) systems in Fukushima accidents and extend BWR RCIC and PWR AFW (Auxiliary Feed Water) operational range and flexibility, mechanistic models for the Terry turbine, based on Sandia National Laboratories' original work, have been developed and implemented into the RELAP-7 code to simulate the RCIC system. This paper presents a set of analytical models for simulating the flow through the Terry turbine nozzles when inlet fluid is pure steam. In the Sandia model, the turbine bucket inlet velocity is provided according to a reduced-order model which was obtained from a large number of CFD simulations. In this work, we propose an alternative method, using an under-expanded jet model to obtain the velocity for the turbine bucket inlet. The models include both adiabatic expansion process inside the nozzle and free expansion process outside of the nozzle to reach the ambient pressure. The combined models are able to predict the steam mass flow rate and supersonic velocity to the Terry turbine bucket entrance, which are the necessary input conditions for the Terry Turbine rotor model. The nozzle analytical models were validated with experimental data and benchmarked with CFD simulations. The analytical models generally agree well with the experimental data and CFD simulations. The analytical models are suitable for implementation into a reactor system analysis code or severe accident analysis code as part of the mechanistic and dynamical models to understand the RCIC behaviors. The scenarios with two-phase flow at the turbine inlet will be pursued in future work.

I. INTRODUCTION

All BWR RCIC (Reactor Core Isolation Cooling) systems and PWR AFW (Auxiliary Feed Water) systems use Terry turbine. The Terry turbine, as shown in Fig. 1, is essentially a solid cylindrical wheel with multiple machined semi-circular 'buckets' that are shaped into the body of the wheel. Fixed nozzles and reversing chambers surrounding the wheel are inside the turbine casing. High pressure steam is accelerated to supersonic flow inside the turbine nozzle. The kinetic energy is then converted to shaft work by the impulse force on the turbine buckets.

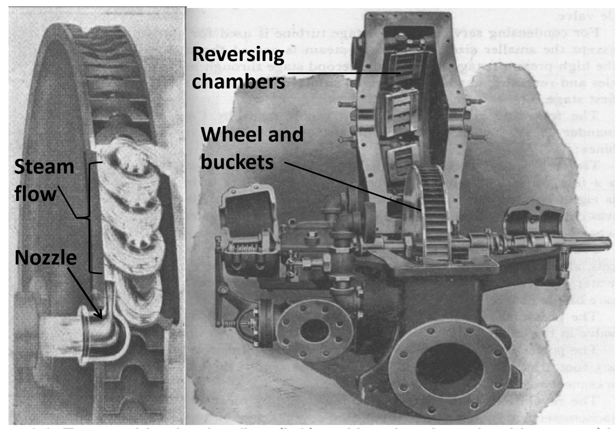

Fig. 1. Terry turbine bucket flow (left) and interior view of turbine case (right) (Ref. 1).

As part of the efforts to understand the unexpected "self-regulating" mode of the RCIC systems in Fukushima accidents and extend BWR RCIC and PWR AFW operational range and flexibility, mechanistic models for the Terry turbine are being developed and implemented into reactor system analysis or severe accident codes, with the funding support from Reactor Safety Technology Pathway of U.S. Department of Energy (DOE)'s Light Water Reactors Sustainability (LWRS) Program (Ref. 1). A set of Terry turbine models suitable for system code implementation had recently been developed by Sandia National Labs (Ref. 1). The Sandia Terry turbine model is based on the following assumptions:

- RCIC uses a single-stage Terry impulse turbine that functions according to the exchange of momentum and kinetic energy.
- Steam enters semi-circular buckets and reverses direction (~180°).
- The reversing chambers are only important for low speed operation, such as during the initial startup.

- The expansion of steam after the nozzles is total; the expansion process converts the static pressure (enthalpy energy) of the steam into kinetic energy to be imparted into the turbine buckets. No meaningful reaction force is developed by the Terry turbine.

The Sandia Terry turbine model is composed of a turbine nozzle model and a turbine rotor model. For the Sandia turbine nozzle model, the turbine bucket inlet velocity is provided according to a reduced-order model which was obtained from a large number of CFD simulations. This reduced-order model is only valid for the specific nozzle design and operation conditions for which the CFD simulations covered.

In the Sandia work, the authors discussed three ways to obtain the turbine bucket inlet velocity information:

1. Developing a sub-model for the system analysis, based on an abstraction of the full pertinent physics, that can calculate the nozzle velocities based on other plant-level predictions;
2. Table lookup of CFD results as a function of various plant variables; or
3. Analytic formula fit of CFD results as a function of various plant variables.

The third option was used for the initial application of the CFD insights into the system models in the Sandia report. In this work, we take the first option to develop a simple analytical model for calculating the entrance velocity to the turbine bucket.

We propose an under-expanded jet model to obtain the velocity and thermodynamic conditions for the turbine bucket inlet. These sets of analytical models are simple and generic, and suitable for use in system analysis codes. The analytical models are valid for any Terry turbine nozzle designs as long as the turbine inlet is pure steam. For two-phase inlet conditions, the current models should be further modified and improved. The models were implemented into the RELAP-7 code. RELAP-7 is a new reactor system code currently under development with the funding support also from US DOE's LWRS Program (Ref. 2). The RELAP-7 code is a fully implicit code and the preconditioned Jacobian-free Newton-Krylov (JFNK) method (Ref. 3) is used to solve the discretized nonlinear system.

A Fully implicit and strongly coupled RCIC system model has been developed in the RELAP-7 code and used for simplified BWR SBO (Station Black-Out) simulations in the past (Refs. 4-7). In this model, a generic turbine model was used to conserve mass and energy while turbine operation characteristic curves were used to obtain non-dimensional mass flow rate and thermal efficiency. This model could be used for simulating RCIC off-design behavior if off-design operation characteristic curves were available. However, No such curves currently exist for the Terry turbine system due to its unique pure impulse design. The modified Sandia Terry turbine model provides a more mechanistic method to simulate the RCIC turbine.

Section II describes the analytical nozzle models. Section III discusses the implementation of the models into the RELAP-7. Section IV presents the benchmark results with experimental data and Sandia's CFD results.

II. ANALYTICAL NOZZLE MODELS

As noted in the Sandia report (Ref. 1), even relationships for ideal gases yield good estimates for the choking mass flow rate for saturated steam, which is not an ideal gas. For the RCIC turbine operating near its design operation condition (saturated steam at high pressure), we postulate that treating saturated steam as an ideal gas would result in sufficiently accurate results for RCIC turbine simulation in a system code. Further extending the idea, the under-expanded or over-expanded jet outside of the nozzle can also be treated as ideal gas. For off-design working conditions, a simple two-phase model can be used to replace the ideal gas model, which will be pursued in the future work.

Fig. 2 shows that the jet flow through a converging-diverging nozzle can be characterized with four distinct stages: (1) adiabatic expansion to sonic condition at the throat from the source and adiabatic expansion to supersonic condition in the expansion part of the nozzle; (2) adiabatic free expansion and reaching the ambient pressure (virtual nozzle); (3) zone of flow establishment (ZOFE); (4) free jet. Different models are used for analyzing each stage. As discussed in the Sandia report, the jet enters the bucket near the maximum speed, where the jet static pressure is equal to the turbine ambient pressure. The jet should be at the stage of the zone of flow establishment or near the end of the virtual nozzle. Therefore, the free jet model is irrelevant in the simulation and is skipped in this report. The models for stage 1 to 3 will be discussed here.

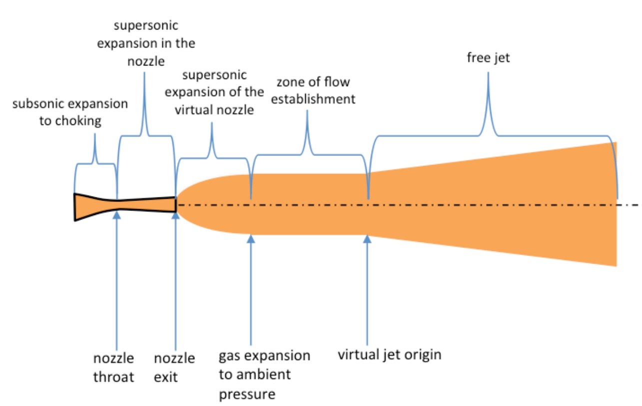

Fig. 2. Schematic of high pressure gas flow through a nozzle.

For the adiabatic expansion process from the source to the nozzle throat, an isentropic process is assumed and the choking is assumed to happen at the throat point. When the ideal gas law is assumed, the choking mass flow rate, pressure, and temperature can be calculated according to the source conditions (Refs. 8, 9).

$$\dot{m}_c = \mathrm{A_t}(\rho u)_c = A_t(\gamma p_c \rho_c)^{1/2} \tag{1}$$

where $\mathrm{A_t}$ is the cross-section area at the nozzle throat. The critical pressure p_c and the critical density ρ_c are calculated by

$$\frac{p_c}{p_{10}} = \left(\frac{2}{\gamma+1}\right)^{\frac{\gamma}{\gamma-1}} \tag{2}$$

$$\frac{\rho_c}{\rho_{10}} = \left(\frac{2}{\gamma+1}\right)^{\frac{1}{\gamma-1}} \tag{3}$$

where the subscript '*10*' indicates the stagnation condition for the inlet. To derive stagnation states, we first have

$$h_0 = h + \frac{1}{2}u^2 \tag{4}$$

where u is the velocity. Assuming an isentropic process, from the static state, say, (h_1, p_1), we can find the stagnation state (h_{01}, p_{01}). For an ideal gas, the following equations hold (Ref. 9)

$$p_0 = p\left(1 + \frac{\rho u^2}{2p} \cdot \frac{\gamma-1}{\gamma}\right)^{\gamma/(\gamma-1)} \tag{5}$$

$$T_0 = T\left(\frac{p_0}{p}\right)^{(\gamma-1)/\gamma} \tag{6}$$

$$\rho_0 = \frac{p_0}{RT_0} \tag{7}$$

where R is the gas constant.

From the nozzle throat to the nozzle exit, an adiabatic supersonic expansion process is assumed. According to the model summarized by NASA (Ref. 10), the Mach number (M) at any point of the nozzle between the throat and the exit can be calculated by the following equation:

$$\frac{A}{A_t} = \left(\frac{\gamma+1}{2}\right)^{-\frac{\gamma+1}{2(\gamma-1)}} \frac{\left(1+\frac{\gamma-1}{2}M^2\right)^{\frac{\gamma+1}{2(\gamma-1)}}}{M} \tag{8}$$

where A is the cross-section area at any location of the nozzle, A_t the throat area, and γ the ratio of specific heats. Note that this is a nonlinear equation and a nonlinear solver is needed. When the Mach number is available, the pressure, temperature, density, and velocity can be calculated according to the following equations, respectively:

$$\frac{p}{p_0} = \left(1 + \frac{\gamma-1}{2}M^2\right)^{-\frac{\gamma}{\gamma-1}} \tag{9}$$

$$\frac{T}{T_0} = \left(1 + \frac{\gamma-1}{2}M^2\right)^{-1} \tag{10}$$

$$\frac{\rho}{\rho_0} = \left(1 + \frac{\gamma-1}{2}M^2\right)^{-\frac{1}{\gamma-1}} \tag{11}$$

The sound speed is calculated as:

$$a = \sqrt{\gamma RT} \tag{12}$$

and velocity is calculated from:

$$u = Ma \tag{13}$$

With Eqs. (8) to (13), the flow conditions at the nozzle exit can be calculated.

For the non-isentropic adiabatic free expansion process from the nozzle exit to the point where the pressure decreases to the ambient value, pressure, temperature, velocity, and density vary rapidly while the jet diameter expands significantly over a short distance from the nozzle exit (Ref. 11). This process is called virtual nozzle in literature, as shown in Fig. 3.

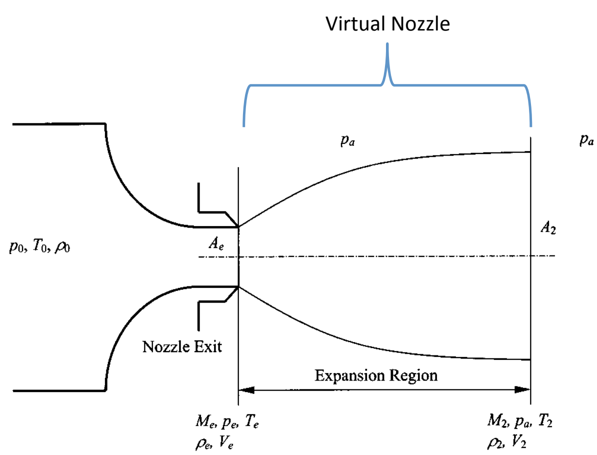

Fig. 3. Schematic depicting of the virtual nozzle process of an under-expanded jet (Ref. 11).

The mass entrained by the jet during this expansion process is insignificant compared to the jet mass flow rate from the nozzle exit. Therefore, it is assumed that there is no mass flux through the jet boundary at this stage. According to mass, momentum, energy balances and the ideal gas law, four equations can be formulated to calculate jet velocity, temperature, density, and diameter at the end of this stage. This method has been used by

Xiao et al. (Ref. 12) and Bulent Yuceil et al. (Ref. 11). The following summarizes the model:

$$u_v = \frac{p_e - p_v + \rho_e u_e^2}{\rho_e u_e} \tag{14}$$

$$T_v = T_e + \frac{u_e^2 - u_v^2}{2c_p} \tag{15}$$

$$\rho_v = \frac{\rho_e T_e}{p_e} \frac{p_v}{T_v} \tag{16}$$

$$d_v = d_e \sqrt{\frac{\rho_e u_e}{\rho_v u_v}} \tag{17}$$

Where subscript v represents the location at the end of the virtual nozzle and e represents the location at the nozzle exit, and d is the diameter.

In order to estimate the length of this stage, the distance for the Mach disk, where the shock occurs, is assumed to approximate this expansion length. The model developed by Velikorodny and Kudriakov (Ref. 13) is used in this paper to calculate the distance for the Mach disk:

$$\frac{x_v}{d_e} = \frac{1}{2} \sqrt{\frac{\gamma P_e}{P_\infty}} \left(\frac{\gamma+1}{\gamma-1}\right)^{1/4} \tag{18}$$

Where d_e is the nozzle exit diameter, P_e the pressure at the nozzle exit, and P_∞ the ambient pressure.

The zone of flow establishment describes the process where unsheared jet profiles undergo changes into profiles with similarity. The transition is complex and the transition length has large uncertainty. For low-speed flow, the distance extends up to 5-10 times the orifice diameter (Ref. 14). For sonic or supersonic flow, the length is even larger. According to the experimental results presented by Bulent Yuceil (Ref. 11), the temperature profiles became self-preserving at about 18 jet diameters at the end of the virtual nozzle for the studied cases.

Given upstream conditions, this set of models calculates the Terry turbine bucket inlet conditions such as velocity and mass flow rate. These inputs are used to close the angular momentum equation for the turbine rotor.

III. IMPLEMENTATION OF THE NOZZLE MODELS INTO RELAP-7

The RELAP-7 code is being developed based on the MOOSE (the Multi-Physics Object-Oriented Simulation Environment) framework (Ref. 15), which provides software development environment and computational framework for RELAP-7. Like all other reactor system analysis codes, the RELAP-7 thermal hydraulics model is composed of a network of one-dimensional (1-D) physical components connected by zero-dimensional (0-D) physical components. There are three main types of components developed in RELAP-7: 1-D components, 0-D components for setting boundary conditions (BC) for the 1-D components, and 0-D components for connecting 1-D components and describing additional 0-D averaged physics processes. 1-D components, such as pipe, heat exchanger, and core channel, describe 1-D fluid flow model and additional heat conduction model. Zou et al. (Ref. 16) described the single-phase fluid flow model and several 1-D component models developed for RELAP-7. The Terry turbine nozzle models are implemented as a simple 0-D component.

MOOSE uses pre-conditioned JFNK method to solve the nonlinear system in the residual form:

$$\boldsymbol{F}(\boldsymbol{U}) = 0 \tag{19}$$

for the unknown vector $\boldsymbol{U}$. Each component of the $\boldsymbol{F}$ vector represents one discretized residual equation. The solution to the nonlinear system is obtained by iteratively solving a series of Newton's linear correction equations,

$$\boldsymbol{J}(\boldsymbol{U}^k)\delta\boldsymbol{U}^k = -\boldsymbol{F}(\boldsymbol{U}^k) \tag{20}$$

where $\boldsymbol{J}(\boldsymbol{U}^k)$ is the Jacobian matrix, the (i, j) element (ith row, jth column) of the Jacobian matrix is

$$J_{ij} = \frac{\partial F_i(\boldsymbol{U})}{\partial u_j} \tag{21}$$

$\boldsymbol{U}^k$ is the k^{th} nonlinear step solution; and $\delta\boldsymbol{U}^k$ is the correction vector. In the JFNK frame, the linear system, equation (20), could be effectively solved with a Krylov's method. In the Krylov's method, only a matrix-vector product is required and thus it does not require the explicit formation of the Jacobian matrix. The matrix-vector product can be approximated as,

$$\boldsymbol{J}(\boldsymbol{U}^k)\boldsymbol{v} \approx \frac{\boldsymbol{F}(\boldsymbol{U}^k + \epsilon\boldsymbol{v}) - \boldsymbol{F}(\boldsymbol{U}^k)}{\epsilon} \tag{22}$$

in which, $\boldsymbol{v}$ is the Krylov vector and ϵ is a small perturbation parameter. After the correction vector, $\delta\boldsymbol{U}^k$, is solved from the linear system, the $(k+1)^{\text{th}}$ nonlinear step solution could be updated as,

$$\boldsymbol{U}^{k+1} = \boldsymbol{U}^k + \delta\boldsymbol{U}^k \tag{23}$$

For the Terry turbine nozzle component, we defined the inlet pressure and the nozzle outlet Mach number as the two primary unknowns. The inlet pressure unknown corresponds to the mass conservation equation for the inlet:

$$(\rho uA)_1 - \dot{m}_c = 0 \qquad (24)$$

where $(\rho uA)_1$ is the coupled mass flow rate variable at the inlet pipe end and $\dot{m}_c$ is calculated according to Eq. (1). The Mach number unknown corresponds to Eq. (8). Analytical Jacobians for Eq. (24) and Eq. (8) with respective to all the primary unknowns are provided so that efficient pre-conditioning method can be used. Major parameters at the nozzle outlet and at the end of the virtual nozzle are defined as auxiliary variables, which can be calculated from the primary variables according to Eqs. (2) to (7) and Eqs. (9) to (18).

IV. BENCHMARK WITH EXPERIMENTAL DATA AND SANDIA CFD RESULTS

A test case as shown in Fig. 4 is established. In this model, the pipe upstream boundary conditions such as pressure and temperature are set in the Time Dependent Volume component. For the Terry turbine nozzle component, the required parameters include: throat area, exit area, and the nozzle outlet ambient pressure. The important outputs include the choked mass flow rate through the system, velocities at the nozzle exit and at the end of the virtual nozzle, and the virtual nozzle length. Since all the tests involve supersonic high speed flow, a small time step 0.01 second is used.

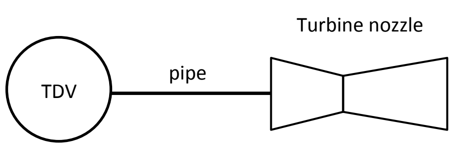

Fig. 4. RELAP-7 nozzle test case.

IV.A. Benchmark With Steam Nozzle Experiments

The same steam nozzle experiment used for benchmark in the Sandia research (Ref. 1) was used for validating the proposed analytical model and comparing with Sandia CFD results. Fig. 5 shows the test nozzle geometry. This nozzle test only had in-nozzle data. The analytical model assumes dry saturated steam at the nozzle inlet. The thermodynamic constants in the model are evaluated from realistic steam properties and are kept constant through the expansion process.

Fig. 6 compares the velocity values calculated with the analytical model against the CFD results from the Sandia team and test data. Note that the nozzle test data reflects conditions just before the exit (near 90% nozzle length) while all the calculation results are at the nozzle exit. It can be seen that the simple analytical model results match the CFD results very well and both analytical model results and CFD results reasonably agree well with the test data except for the low pressure steam jet test point. The reason for the discrepancy is due to the fact that shocks develop in the diverging section of the nozzle for the lower inlet pressure cases as revealed by the test data and CFD simulations. The simple analytical model cannot account for the situation with shocks appearing inside the nozzle. Shocks in the diverging section are indicative of over-expanded nozzle flow, which results from too low of a pressure drop over the nozzle geometry. However, over-expanded flow is not anticipated for the Terry turbine nozzles, given the high reactor vessel (or steam generator) pressures for such applications. Higher inlet pressures will push shocks out of the nozzle and result in under-expanded flow (Ref. 1). From the test nozzle benchmark, we conclude that the simple analytical model can predict similarly accurate nozzle exit velocity as the complex CFD models do.

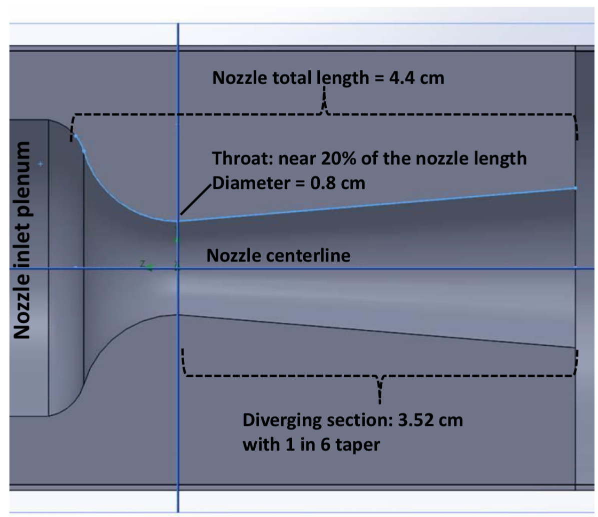

Fig. 5. Test nozzle geometry (Ref. 1).

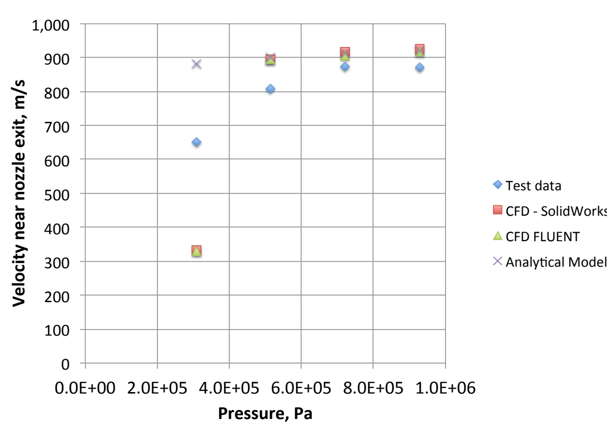

Fig. 6. Velocities near test nozzle exit.

IV.B. Terry Turbine Nozzle Results And Comparison With CFD Results

The Terry turbine geometry specified by the Sandia study (Ref. 1), as shown in Table I, is used for the Terry turbine benchmark study. In this section, the Sandia CFD results will be used for benchmarking the analytical model. It is noted that the nozzle length is very short and there is a 1.5 cm gap between the nozzle exit and the turbine bucket entrance. Therefore this case is not only good for verifying the nozzle expansion model, but also useful for checking the virtual nozzle model for either the under-expanded or over-expanded jets.

TABLE I. Terry Turbine Geometry (Ref. 1)

Model Variable	Quantity
Turbine wheel diameter	61 cm (24 inches)
Turbine wheel and bucket width	7 cm
Number of nozzles and reversing chamber sets	5
Number of reversing chambers per nozzle set	4
Number of buckets on wheel	84
Nozzle length	1.7 cm
Nozzle circular throat diameter	0.56 cm
Nozzle square exit side length	0.64 cm
Distance from nozzle exit to bucket entrance	≈1.5 cm

Fig. 7 shows the mass flow rates through the nozzle under different upstream pressures. The analytical model results agree well with the Sandia FLUENT CFD results. The relative errors are about 10%. This error range should be in the uncertainty range for either CFD methods or the analytical method.

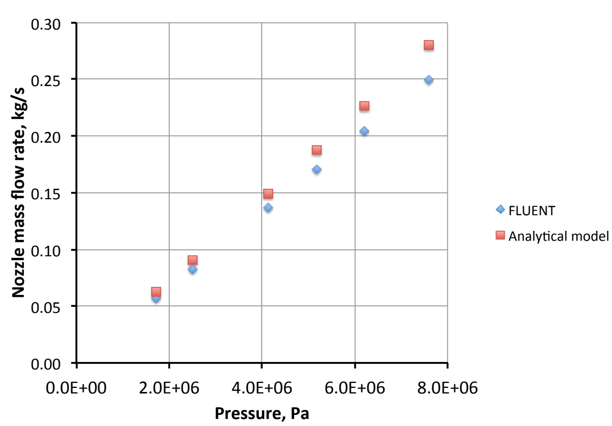

Fig. 7. Comparisons of Nozzle mass flow rates calculated from the analytical model and from the Sandia FLUENT model.

Fig. 8 shows the virtual nozzle lengths for two different outlet pressures under different inlet pressures. The RCIC turbine typically operates under high inlet pressure (i.e. between 6 to 8 MPa). For those situations, the virtual nozzle lengths are typically slightly larger than the gap distance between the nozzle exit and the entrance to the bucket (1.5 cm). Therefore, the jet velocity at the end of the virtual nozzle is a good approximation for the bucket entrance velocity.

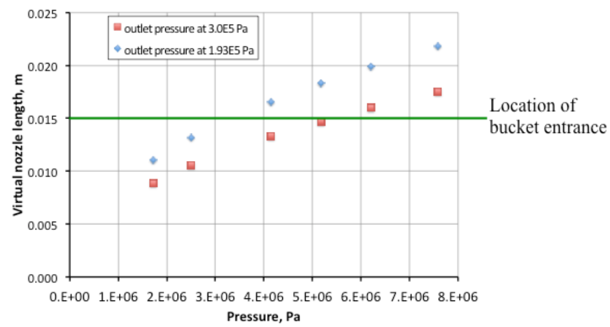

Fig. 8. Virtual nozzle length (from the nozzle exit to the end of virtual nozzle).

Fig. 9 and Fig. 10 show the bucket entrance velocities for the two outlet pressures. The analytical model generally predicts higher entrance velocities than the Sandia CFD model. The CFD simulations show condensation near the bucket entrance, which results in lower velocities. The analytical model cannot account for this effect therefore results in higher velocities. For the high inlet pressure operation range typical for RCIC turbine (6 – 8 MPa), the analytical model and CFD results are close: less than 15% errors for the high outlet pressure case and less than 3% errors for the low outlet pressure case. When the inlet pressure is lower than 5 MPa, the prediction difference between the analytical model and the Sandia CFD model becomes larger. However, both models predict similar trends. The RCIC system typically only experiences low inlet pressure during the short period of the primary system depressurization process. The RCIC system behavior during depressurization is not important to the system response due to large amount of steam release through SRVs (Safety/Relief Valve). Considering these facts, the larger difference in the bucket entrance velocity for lower inlet pressure cases should not be a big concern in terms of the overall RCIC simulation uncertainty.

When the DC power for controlling the RCIC system is lost, the RCIC turbine would operate either in two-phase mode or periodically experiencing liquid water or two phase mode. An effective two phase analytical model is necessary to capture the major physics for this off-design mode, which is only possible to be further developed after enough experimental data becomes available in the near future.

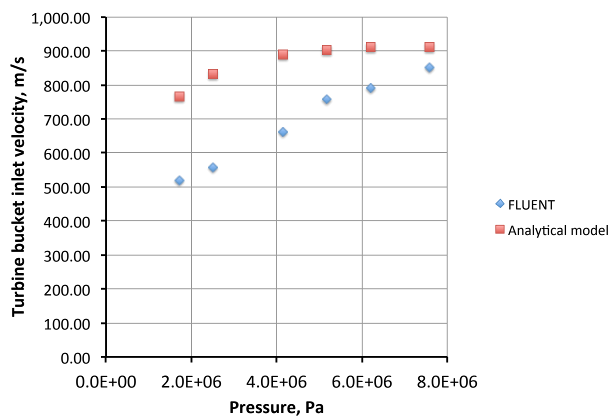

Fig. 9. Turbine bucket inlet velocity for the high outlet pressure case (3.0E5 Pa).

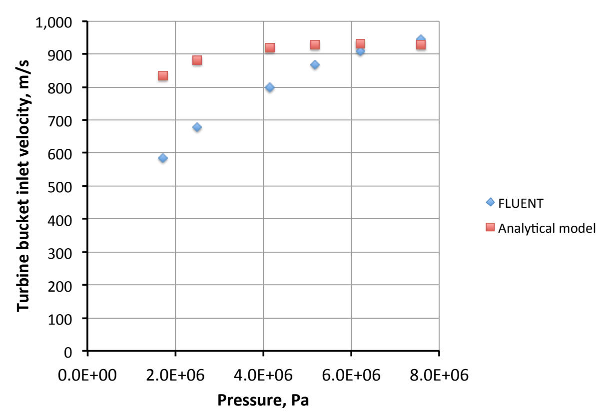

Fig. 10. Turbine bucket inlet velocity for the low outlet pressure case (1.93E5 Pa).

V. CONCLUSIONS

This paper summarizes a set of analytical models for the Terry turbine nozzle. The models include both adiabatic expansion process inside the nozzle and free expansion process outside of the nozzle to reach the ambient pressure. The combined models are able to predict the steam mass flow rate and supersonic velocity to the Terry turbine bucket entrance, which are the necessary input information for the Terry Turbine rotor model. The nozzle analytical models were validated with experimental data and benchmarked with CFD simulations. The analytical models generally agree well with the experimental data and CFD simulations. The analytical models are suitable for implementation into a reactor system analysis code or severe accident analysis code as part of mechanistic dynamical models to understand the RCIC behaviors.

NOMENCLATURES

a	sound speed
c_p	specific heat at constant pressure
d	diameter
h	enthalpy
$\dot{m}$	mass flow rate
p	pressure
u	velocity
$\boldsymbol{v}$	Krylov vector
A	area
$\boldsymbol{F}$	residual vector
$\boldsymbol{J}$	Jacobian matrix
M	Mach number
R	gas constant
T	temperature
$\boldsymbol{U}$	unknown vector

Greek

γ	the ratio of the specific heats
ε	perturbation parameter
ρ	density

Subscript

c	critical
e	nozzle exit
t	throat
v	virtual nozzle exit
0	stagnation
1	inlet
∞	ambient

ACKNOWLEDGMENTS

This work is supported by the U.S. Department of Energy, under Department of Energy Idaho Operations Office Contract DE-AC07-05ID14517. Accordingly, the U.S. Government retains a nonexclusive, royalty-free license to publish or reproduce the published form of this contribution, or allow others to do so, for U.S. Government purposes.

REFERENCES

1. K. ROSS, et. al., *Modeling of the Reactor Core Isolation Cooling Response to Beyond Design Basis Operations – Phase 1*, SAND2015-10662, December, (2015).
2. H. Zhang, et. al., *RELAP-7 Development Updates*, INL/EXT-15-36763, September, (2015).

3. D. A. KNOLL and D. E. KEYES, "Jacobian-free Newton-Krylov Methods: a Survey of Approaches and Applications", *J. Comp. Phys.*, **193**, 357-397 (2004).
4. H. ZHAO, et. al., "Developing Fully Coupled Dynamical Reactor Core Isolation System Models in RELAP-7 for Extended Station Black-Out Analysis," *Proceedings of 2014 International Congress on Advances in Nuclear Power Plants*, Charlotte, North Carolina, USA, April 6-9, (2014).
5. H. ZHAO, et. al., *Refined Boiling Water Reactor Station Blackout Simulation with RELAP-7*, INL/EXT-14-33162, September, (2014).
6. H. ZHAO, et. al., "Demonstration of Fully Coupled Simplified Extended Station Black-Out Accident Simulation with RELAP-7," *Proceedings of PHYSOR 2014 – The Role of Reactor Physics Toward a Sustainable Future*, Kyoto, Japan, September 28 – October 3, (2014).
7. H. ZHAO, et. al., "A Strongly Coupled Reactor Core Isolation Cooling System Model for Extended Station Black-Out Analyses," *Proceedings of the 16th International Topical Meeting on Nuclear Reactor Thermal Hydraulics (NURETH-16)*, Hyatt Regency Chicago, USA, August 30-September 4, 2015.J. GLEASON, "Format for a Report," ANS-2008, American Nuclear Society (2008).
8. S. LEVY, *Two-phase flow in complex systems*. John Wiley & Sons, page 303 to 305, (1999).
9. HIH. SARAVANAMUTTOO, et. al., *Gas Turbine Theory*, 5th edition, pp. 54-56, Pearson Education Limited, (2001).
10. T. BENSON, *Isenotropic Flow*. http://www.grc.nasa.gov/WWW/k-12/airplane/isentrop.html. National Aeronautics and Space Administration. 21 June 2014. Accessed March 24, (2016).
11. K. BULENT YUCEIL and M. VOLKAN OTUGEN, "Scaling Parameters for Underexpanded Supersonic Jets," *Physics of Fluids*, **14**, 4206, (2002).
12. J. XIAO, J. R. TRAVIS, W. BREITUNG, "Hydrogen release from a high pressure gaseous hydrogen reservoir in case of a small leak," *International Journal of Hydrogen Energy*, **36**, 2545-2554, (2011).
13. A. VELIKORODNY and S. KUDRIAKOV, "Numerical Study of the Near-Field of Highly Under-Expanded Turbulent Gas Jets", *Proc. of ICHS 2011*, (2011).
14. GH. JIRKA, "Integral model for turbulent buoyant jets in unbounded stratified flows. Part I single round jet." *Environmental Fluid Mechanics*, **4**, pg 1-56, (2004).
15. D. GASTON, et. al., "MOOSE: A Parallel Computational Framework for Coupled Systems of Nonlinear Equation", *Nuclear Engineering Design*, **239**, 1768-1778, (2009).
16. L. ZOU, et al., "Solving Multi-Mesh Flow and Conjugate Heat Transfer Problems with RELAP-7," *Proc. of the International Conference on Mathematics and Computational Methods Applied to Nuclear Science & Engineering (M&C 2013)*, Sun Valley, Idaho, USA, May 5-9, (2013).